Allosteric Modulation of PCSK9-LDLR Interaction: Can Structureless Loops be Drug Targets?

Ipsita Basu,[a,‡], Krishnendu Sinha,[a,‡], Zacharia Shah,[b] Salim Shah,[b] and Suman Chakrabarty[a,*]

[a] Department of Chemical and Biological Sciences, S. N. Bose National Centre for Basic Sciences, Kolkata – 700 106, India
[b] Hingez Therapeutics Inc, USA

ABSTRACT: While most of the drugs available in the market are competitive inhibitors, there is a rapidly growing interest in development of allosteric drugs, particularly to inhibit protein-protein interactions (PPI) with large interaction surface area. However, it remains a challenge to identify a distal binding site that would be allosterically linked to the canonical ligand/substrate binding site. Such allosteric hotspots are often cryptic sites with a less populated excited conformational state of the protein. In this work we present a general strategy based on thermodynamic arguments to identify such distal cryptic sites as potential targets for allosteric drugs. We demonstrate this on allosterically modulating the PPI between PCSK9 (proprotein convertase subtilisin/Kexin type 9) and LDLR (low density lipoprotein receptor), which is a challenging and therapeutically important target towards treatment of hypercholesterolemia (elevated plasma level of LDL). Using several μs long molecular dynamics (MD) simulations, we demonstrate that on binding with the EGF-A domain of LDLR, there is a significant conformational change (population shift) in a distal loop (residues 211-222) region of PCSK9. We have identified several (meta)stable and kinetically resolved conformational states of this loop and demonstrated that there exists a clear correlation between the loop conformation and the binding affinity with LDLR. Using a thermodynamic argument, we establish that the loop conformations predominantly present in the apo state of PCSK9 would have lower binding affinity with LDLR and they would be potential targets for designing allosteric inhibitors. We also elucidate the molecular origin of the allosteric coupling between this loop and PCSK9-LDLR binding interface in terms of population shift in several specific pair-wise interactions consisting of salt bridges and hydrogen bonds. Overall, our work provides a general strategy towards identifying allosteric hotspots, where one should compare the conformational ensemble between the apo and substrate bound states of the protein and identify distal differences, if any. Subsequently the apo-like conformations should be targeted for designing inhibitors that would specifically bind to those conformations and stabilize them.

Cardiovascular diseases continue to be the leading cause of death worldwide. They are usually associated with a buildup of plaque on the interior wall of the arteries (atherosclerosis). The primary risk factors for atherosclerosis include elevated plasma levels of triglycerides, low-density lipoprotein (LDL)-cholesterol (LDL-c; hypercholesterolemia), diabetes, high blood pressure etc. While statins are being widely used to treat hypercholesterolemia, many patients experience rhabdomyolysis or insufficient efficacy, especially those who have very high baseline LDL-c. Recently, PCSK9 (proprotein convertase subtilisin/Kexin type 9) has been discovered as a new member of lipid metabolism and is pursued as a new target to treat hypercholesterolemia.[1-5] PCSK9 competes with LDL-c to bind to LDL receptors (LDLR). More importantly, unlike LDL-c/LDLR interactions, where LDLR recycles back to the cell surface, PCSK9/LDLR interactions lead to degradation of LDLR and decreasing LDLR density. This double whammy is obvious in patients who have the gain-of-function mutation PCSK9 (familial hypercholesterolemia). These patients have very high levels of LDL-c and die at a young age due to cardiovascular complications. Thus, the main therapeutic goals are either to reduce circulating PCSK9 or block its interactions with LDLR.[6-13] The former goal is successfully achieved with monoclonal antibodies (Repatha), and other approaches such as siRNA and gene silencing are underway.[14] However, these therapeutic modalities have limited access because of cost, manufacturing challenges, and scanty safety data. Oral small molecule therapeutic approaches have proven to be most accessible and cost-effective. But developing a small molecule to block protein-protein interactions between PCSK9 and LDLR is difficult. The binding surface is very large (>500 Å^2) and is relatively flat. Two main approaches are pursued to block PPIs- (1) hotspot; and (2) allostery. The former approach relies on the fact that some spots on the PPI surface act as anchors. Disrupting these anchors either weakens or entirely unravels the entire PPI. The latter approach has been known, in some form, for decades (e.g., Hemoglobin cooperative binding or ATP-mediated inhibition of phosphofructokinase). However, most of these cases involve a well-defined active site to accommodate small molecule modulators. Disrupting PPIs allosterically with a small molecule is a novel concept and is an active area of research.[15-21]

Recent studies have reported some preliminary success in allosterically disrupting PCSK9-LDLR PPIs, where druggable binding sites are located far from the PCSK9-LDLR interaction surface, and potential inhibitors have been identified using virtual screening and in vitro binding assays.[12,22] However, the search for such allosteric sites is somewhat ad hoc because these sites only opened up, as low-lying, metastable states, in molecular dynamics experiments but were otherwise unavailable in crystal structures. Moreover, the mere identification of a distal small molecule binding site is not sufficient unless they are allosterically (thermodynamically) coupled to the PCSK9-LDLR binding interface. In this work, we propose a general design

strategy to identify the allosteric sites based on thermodynamic arguments. Specifically, we demonstrate that the structural plasticity of certain disordered loop regions in PCSK9 may be exploited as promising drug binding sites and to disrupt PCSK9-LDLR interactions.

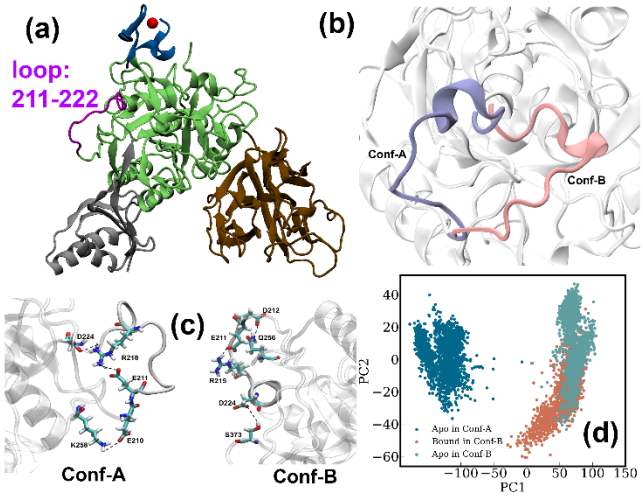

Figure 1. (a) Crystal structure of PCSK9:EGF-A complex (PDB ID: 4NE9): Pro-domain (residue 61-152): silver, Catalytic domain (residue 153-451): green, C-terminal domain (residue 452-682): brown, and the EGF-A domain of LDLR: blue. (b) Superposition of the representative conformations of the loop 211-222 from the most populated clusters from the apo (Conf-A; ice blue) and EGF-A bound (Conf-B; pink) trajectories. (c) Specific interactions (salt bridges and hydrogen bonds) stabilizing the conformations (Conf-A and Conf-B). (d) Principal Component Analysis (PCA) to characterize the conformational space explored by the loop 211-222: The trajectories projected on the top two PCs (PC1 and PC2) are: (i) apo (dark blue dots), (ii) bound (salmon dots), and (iii) apo in Conf-B (light blue dots) obtained after deleting the EGF-A domain from the bound structure.

PCSK9 is a multi-domain protein (see Fig.1a) consisting of pro-domain (residue 61-152), catalytic domain (residue 153-451) and C-terminal domain (residue 452-682). The catalytic domain primarily interacts with the EGF-A domain of LDLR. The crystal structure used in this study (PDB ID: 4NE9) contains two structures: (i) PCSK9 bound to the EGF-A domain of LDLR and (ii) the apo form. After modelling the missing residues (provided in Table S1 in the SI) of the protein and superimposing the EGF-A bound and apo structures of PCSK9, we noticed that the loop 211-222 has a large difference in conformation between these two states. In Fig. 1b these two extreme conformations are marked as Conf-A (apo) and Conf-B (bound).

In order to ensure that this large change in loop conformation is not an artefact of the homology modeling, we have carried out 2μs long unbiased molecular dynamics (MD) simulations starting from the respective crystal structures. Moreover, to test whether the EGF-A bound conformation is indeed (meta)stable in nature, we have deleted the EGF-A from the bound structure to generate the "apo" state in the originally "bound" conformation (apo state with loop being in Conf-B conformation). Interestingly, in all these three types of trajectories the loop conformation did not interconvert between the conformational states indicating that indeed these are distinct and kinetically resolved at a μs timescale. Representative structures from the most populated clusters obtained from the apo and bound trajectories are shown in Fig.1(b), where Conf-A and Conf-B are the conformations in the "apo" and "bound" states, respectively. In Fig.1(c) we show the distinct set of specific interactions (salt bridges and hydrogen bonds) responsible for stabilizing these two distinct conformations.

In order to characterize the conformational space of the loop sampled in the MD trajectories, we have performed principal component analysis (PCA). Fig. 1d shows the projection of all three trajectories (apo, EGF-A bound, and starting from bound conformation after deleting the EGF-A) on the first two principal components (PC1 and PC2). It is quite evident that the conformational space sampled in the "apo" and "bound" states are different and widely separated. Interestingly, even after deleting the EGF-A domain, the loop conformation remains close to the Conf-B state for the entire duration of the simulation (2μs), and it does not convert to the Conf-A conformation, which is the ground/native state for the apo form. This clearly indicate that the loop 211-222 may exist in at least 2 distinct conformations separated by large free energy barrier, and binding with EGF-A leads to a population shift in the conformational space. This is also supported by Figure S9 in the SI. The free energy barrier separating these conformational states must be large enough such that the timescale of interconversion would be at least several microseconds as indicated from the unbiased MD simulations.

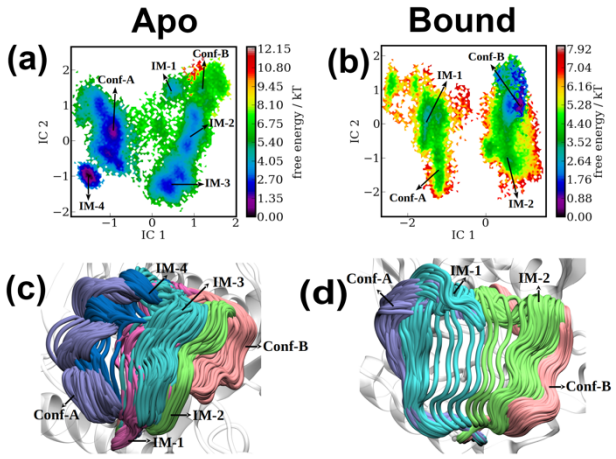

Figure 2. Markov state model (MSM) for the apo (left column) and bound (right column) systems: (top row) Free energy surfaces projected along first two TIC coordinates (IC1 and IC2) for (a) apo and (b) bound; and (bottom row) representative structures from each of macrostates for (c) apo and (d) bound systems. Here we have considered six macrostates for apo (Conf-A, IM-1, IM-2, IM3, IM4 and Conf-B) and four macrostates for bound (Conf-A, IM-1, IM-2 and Conf-B).

Based on the above observations we can safely conclude that the EGF-A binding allosterically coupled to the loop conformation at a distal site (211-222). But in order to compare the relative stability of the distinct conformational states of the loop in the presence and absence of EGF-A domain, we would need to compute the underlying conformational free energy landscape. Given the lack of "structure" in the disordered loop region, it is challenging to define a suitable collective variable

(CV) to describe the conformational space sampled by the loop. Here we have used a set of specific pair-wise contacts that undergo significant changes between the Conf-A and Conf-B as the feature set to build a Markov State Model (MSM) of the conformational states (Table S3 and Figure S5 in the SI). The TIC (time-lagged independent component) projections were used to identify the slowest-relaxing collective degrees of freedom for identifying the macrostates and computing the free energy surfaces.[23-25] The MSM has been built using several short trajectories (200-500ns long) generated in between the extreme structures: Conf-A and Conf-B. The initial configurations for the intermediate structures were generated using steered MD runs. Details of the computational protocol have been provided in the SI.

Figs. 2a and 2b show the conformational free energy landscapes for the apo (without EGF-A) and bound (with EGF-A) systems, respectively, as projected on the first two TIC vectors (IC1 and IC2). Interestingly, both systems show existence of several intermediate conformational states. In particular, both extreme conformations Conf-A and Conf-B exist in both systems, only their relative stability changes on binding with EGF-A. As expected, Conf-A and Conf-B are the global minimum for the apo and bound systems, respectively. This alludes to the conformational selection model of allostery, where several conformational states may pre-exist in a dynamic equilibrium, and the ligand binding may lead to a population shift in the conformational space. The computed free energy landscapes confirm that binding with EGF-A significantly alters the conformational landscape/population of the distal loop 211-222. While Conf-B corresponds to the global minimum in the case of "bound" system, as expected, there exist multiple metastable minima corresponding to the various macrostates: IM-1, IM-2, and Conf-A (Fig. 2b). These are the low-lying metastable states accessible to loop 211-222 even in the presence of the EGF-A domain. We show next that these metastable conformational states could be potential targets to design PCSK9 inhibitors.

So far, we have established that EGF-A binding allosterically modulates the conformational free energy landscape of a distal loop, which may exist in several distinct, metastable and kinetically resolved conformational states. But is the reverse also true? In other words, if we can control/tune the conformation of this loop region, would that modulate the binding affinity of the ligand (EGF-A), which is our therapeutic goal? Fig. 3 shows a schematic thermodynamic cycle to establish this connection. Here we assume that the allosteric site may exist in two (square: S and triangular: T) conformations. The free energy difference between these two conformations (hence, their relative population) depends on the ligand binding status: $\Delta G_{holo}^{S\to T}$ and $\Delta G_{apo}^{S\to T}$ are the free energy differences between the S and T states for the holo and apo, respectively. Also, the ligand binding free energy depends on the conformational state of the allosteric site: ΔG_b^S and ΔG_b^T for the S and T states, respectively. The thermodynamic cycle gives us:

$$\Delta G_b^T = \Delta G_b^S + \left(\Delta G_{holo}^{S\to T} - \Delta G_{apo}^{S\to T}\right)$$

Hence, $\Delta G_b^T > \Delta G_b^S$, if $\Delta G_{holo}^{S\to T} > \Delta G_{apo}^{S\to T}$, which implies that the binding affinity will be lower for that conformation (say, S) which has higher stability in the "apo" state. Connecting this back to the PCSK9 system, since Conf-A conformation has higher stability compared to Conf-B in the apo state, this loop conformation should correspond to a lower PCSK9-LDLR binding affinity.

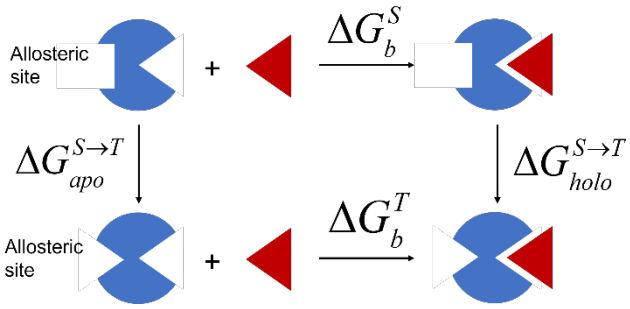

Figure 3. A thermodynamic cycle depicting the dependence of substrate binding affinity on the conformation of a distant allosteric site. The allosteric site may exist in two distinct conformations: square (S) and triangular (T). The S and T conformations are dominant in the ligand (red triangle) bound and apo states, respectively.

In other words, all loop conformations that have higher relative population in the apo state as compared to the EGF-A bound state, should have lower EGF-A binding affinity. Thus, if we can lock those loop conformations using small molecules (inhibitors), our therapeutic goal would be achieved. To validate our hypothesis, we have computed the binding energy between PCSK9 and EGF-A using MM/PBSA method for different conformations of the loop 211-222. We have collected a few hundred structures from each minimum (macrostate) of the free energy surface for the bound system (Fig. 2b) and compared the distribution of the binding energy for those macrostates separately (Fig. 4a). Interestingly, the binding energy distribution shows a systematic shift with the loop conformation following the order Conf-A > IM-1 > IM-2 > Conf-B, which is same as the order of stability of these conformations in the apo form. The average binding energy values are provided in Table S5 in the SI. Hence, we can safely conclude that the loop conformations dominant in the apo form can serve as potential site for designing inhibitors.

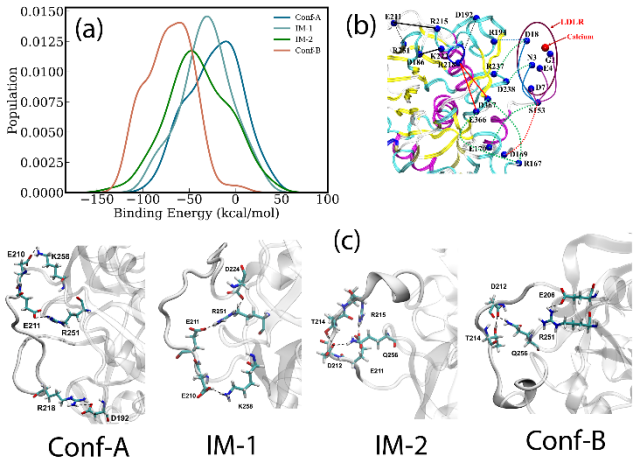

Figure 4. (a) Probability distributions of the MM/PBSA binding energies for the PCSK9-LDLR complex structures obtained from each of the macrostates (minima in free energy surface of bound

system). The average binding energy follows the order: Conf-A < IM2 < IM3 < Conf-B. (b) The network view of perturbation in the pair-wise electrostatic interaction energy, given by: $\Delta E_{ij} = \langle E_{ij} \rangle_{Bound} - \langle E_{ij} \rangle_{Apo}$. The blue spheres indicate residues involved in the allosteric pathway. The lines connecting the pairs of residues with significant energetic perturbation are depicted as follows (in kcal/mol): (i) black: $\Delta E_{ij} < -40$, (ii) purple: $-40 < \Delta E_{ij} < -20$, (iii) red: $-20 < \Delta E_{ij} < -10$, and (iv) green: $-10 < \Delta E_{ij} < -1$. Solid and dashed lines represent the positive and negative values of ΔE_{ij}, respectively. (c) Representative structures for each of the macrostates highlighting the pair-wise specific interactions responsible for stabilization of these conformations.

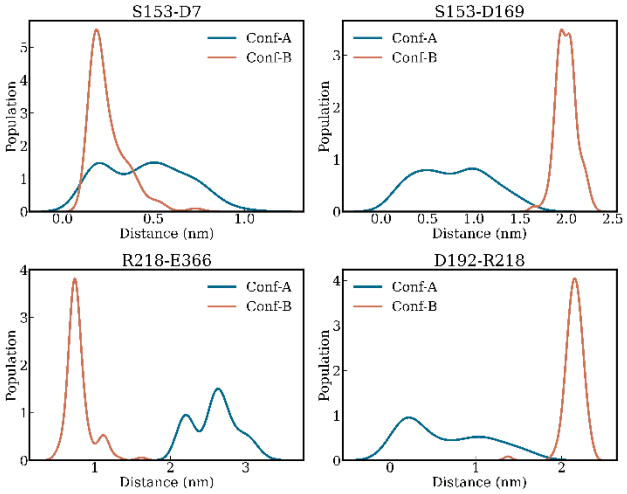

Figure 5. Population distribution of the minimum distance between important residue pairs: (a) S153-D7 (D7 belongs to the EGF-A domain of LDLR), (b) S153-D169, (c) R218-E366, and (d) D192-R218.

Our work also highlights that even a so-called "structureless" or disordered loop may exhibit well-defined and distinct conformational states.[26] Moreover, these specific loop conformations have distinct thermodynamic characteristics in terms of their topology and interactions with rest of the protein. In Fig. 4c, we show that each of these conformational states are stabilized by a set of specific interactions that varies across the conformational states. These interactions are responsible for the kinetic barrier towards interconversion between them. This stability or higher lifetime of these states make them suitable as drug targets.

We have further dissected the molecular origin of the allosteric connectivity between the loop 211-222 and the EGF-A binding interface of PCSK9. In our earlier work we have demonstrated that the non-bonded interaction energy can be a sensitive reporter of subtle conformational changes.[26,27] Using similar ideas, we have built a network of the perturbation in average residue-pair-wise non-bonded interaction energy as follows: $\Delta E_{ij} = \langle E_{ij} \rangle_{Bound} - \langle E_{ij} \rangle_{Apo}$, where $\langle E_{ij} \rangle_{Bound}$ and $\langle E_{ij} \rangle_{Apo}$ are the average non-bonded interaction energy between i-th and j-th residues. In Fig. 4b, we have visualized the connectivity pattern between the residue pairs with large absolute values of ΔE_{ij}. It is fascinating to note that this energetic perturbation map shows a connection between these two distal regions. The ΔE_{ij} values for important residue-pairs are provided in Table S8 in SI.

A close inspection of the ΔE_{ij} values points to a local redistribution of the electrostatic interactions through rearrangement of pair-wise specific interactions. Here are a few examples: residue S153 has a favorable interaction with D169 in Conf-A and this interaction is absent in Conf-B. On the other hand the interaction between S153 and D7 (belongs to the EGF-A domain of LDLR) becomes significantly stronger in the Conf-B. Strengthening of this S153-D7 interaction is consistent with the increase in PCSK9-LDLR binding affinity in the Conf-B. Similarly, another key residue R218 in the loop participates in a strong salt bridge with E366 in Conf-B (absent in Conf-A), whereas it interacts with D192 in Conf-A. In Fig. 5, we illustrate this phenomenon using the probability distribution of the minimum distance between these residue-pairs. A strong peak around 0.2-0.3 nm would correspond to a salt-bridge or hydrogen bond formation.

It is interesting to observe that breaking of one set of favorable interactions in Conf-A is compensated by formation of a different set of interactions in Conf-B. Thus, there are multiple conformational states accessible within close energy range due to this local cancellation or redistribution of the interaction energies. This large conformational entropy associated with the loop conformations seems to be crucial for conformational selection mode of allostery as reported earlier.[28,29] The important role of conformational entropy in allosteric regulation has been highlighted in prior literature as well.[30,31]

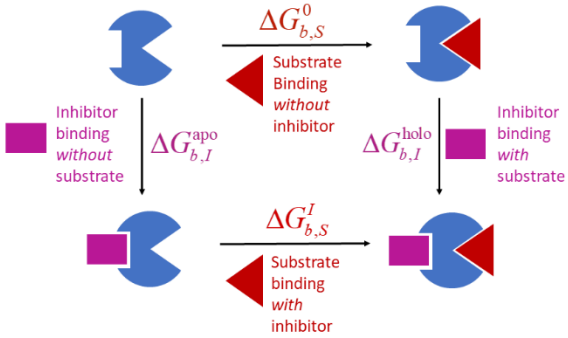

Figure 6. A thermodynamic cycle depicting the mechanism of action of an allosteric inhibitor. The allosteric inhibitor must have different binding affinity depending on the receptor being in the "apo" ($\Delta G^{apo}_{b,I}$) or "holo" ($\Delta G^{holo}_{b,I}$) conformation. $\Delta G^{0}_{b,S}$ and $\Delta G^{I}_{b,S}$ are the substrate binding affinity in the absence and presence of the allosteric inhibitor.

In summary, here we have presented a general framework of identifying potential binding sites for allosterically modulating PPIs. All we need to do is compare the conformational ensemble of the ligand bound and apo forms of the target protein and look for significant conformational changes that exist between the two forms. If such conformations can be found and their thermodynamically distinctiveness can be ascertained either in the apo form or on the liganded form, they can be utilized for virtual screening or structure-based drug discovery. This concept has been schematically proven in the schematic thermodynamic cycle presented in Fig.6. Based on this cycle, we

establish the identity: $(\Delta G^{I}_{b,S} - \Delta G^{0}_{b,S}) = (\Delta G^{\text{holo}}_{b,I} - \Delta G^{\text{apo}}_{b,I})$. Hence, $\Delta G^{\text{holo}}_{b,I} > \Delta G^{\text{apo}}_{b,I}$ would imply $\Delta G^{I}_{b,S} > \Delta G^{0}_{b,S}$. In other words, if the inhibitor (I) has higher binding affinity for the "apo" conformation as compared to the "bound" conformation, then it would imply that the substrate (S) binding affinity would be lower in the inhibitor bound state. We must note that this bidirectional nature of allostery has been discussed earlier in a different context.[16,32]

In this work, we have applied and validated this approach by identifying a distal loop (residues 211-222) in PCSK9 that can allosterically modulate the PCSK9-LDLR interaction through rearrangement and re-wiring of the pair-wise hydrogen bonded network. Our future work will focus on identifying suitable inhibitors targeted to stabilizing the loop conformations with lower binding affinity with LDLR (e.g. Conf-A, IM-1 etc). Moreover, this approach would be tested in other therapeutically important PPI as well towards allosteric drug discovery. Our work presents a counterintuitive view that even disordered loops can have well-defined structure(s) and low-lying metastable conformational states of proteins should be explored in future drug discovery efforts.[26,28,29]

ASSOCIATED CONTENT

Supporting Information. Computational details related to system setup and simulation methods, additional analysis results supporting the observations reported here. Any additional computational data including the MD simulation trajectories may be obtained by contacting the corresponding author.

AUTHOR INFORMATION

Corresponding Author

Suman Chakrabarty
Department of Chemical, Biological & Macromolecular Sciences, S. N. Bose National Centre for Basic Sciences, Kolkata – 700106, India.
Email: sumanc@bose.res.in

Author Contributions

The manuscript was written through contributions of all authors. All authors have given approval to the final version of the manuscript.
‡These authors contributed equally.

Funding Sources

This work has been partially funded by Hingez Therapeutics Inc. and SERB, India (ECR/2018/002903).

Notes

S.S. is the founder of Hingez Therapeutics Inc.

ACKNOWLEDGMENT

I.B. and K.S. thank SNBNCBS for fellowships. Authors thank SNBNCBS for the high-performance computing facility used to carry out the research reported here.

ABBREVIATIONS

PCSK9, Proprotein convertase subtilisin kexin type 9; LDL, low density lipoprotein; LDLR, LDL receptor.

REFERENCES

1 Poirier, S. *et al.* The proprotein convertase PCSK9 induces the degradation of low density lipoprotein receptor (LDLR) and its closest family members VLDLR and ApoER2. *J Biol Chem* **283**, 2363-2372 (2008). https://doi.org:10.1074/jbc.M708098200

2 Cunningham, D. *et al.* Structural and biophysical studies of PCSK9 and its mutants linked to familial hypercholesterolemia. *Nat Struct Mol Biol* **14**, 413-419 (2007). https://doi.org:10.1038/nsmb1235

3 Horton, J. D., Cohen, J. C. & Hobbs, H. H. Molecular biology of PCSK9: its role in LDL metabolism. *Trends Biochem Sci* **32**, 71-77 (2007). https://doi.org:10.1016/j.tibs.2006.12.008

4 Kwon, H. J., Lagace, T. A., McNutt, M. C., Horton, J. D. & Deisenhofer, J. Molecular basis for LDL receptor recognition by PCSK9. *Proc Natl Acad Sci U S A* **105**, 1820-1825 (2008). https://doi.org:10.1073/pnas.0712064105

5 Chan, J. C. *et al.* A proprotein convertase subtilisin/kexin type 9 neutralizing antibody reduces serum cholesterol in mice and nonhuman primates. *Proc Natl Acad Sci U S A* **106**, 9820-9825 (2009). https://doi.org:10.1073/pnas.0903849106

6 Costet, P., Krempf, M. & Cariou, B. PCSK9 and LDL cholesterol: unravelling the target to design the bullet. *Trends Biochem Sci* **33**, 426-434 (2008). https://doi.org:10.1016/j.tibs.2008.06.005

7 Steinberg, D. & Witztum, J. L. Inhibition of PCSK9: a powerful weapon for achieving ideal LDL cholesterol levels. *Proc Natl Acad Sci U S A* **106**, 9546-9547 (2009). https://doi.org:10.1073/pnas.0904560106

8 Seidah, N. G. & Prat, A. The biology and therapeutic targeting of the proprotein convertases. *Nat Rev Drug Discov* **11**, 367-383 (2012). https://doi.org:10.1038/nrd3699

9 Taechalertpaisarn, J., Zhao, B., Liang, X. & Burgess, K. Small Molecule Inhibitors of the PCSK9.LDLR Interaction. *J Am Chem Soc* **140**, 3242-3249 (2018). https://doi.org:10.1021/jacs.7b09360

10 Tucker, T. J. *et al.* A Series of Novel, Highly Potent, and Orally Bioavailable Next-Generation Tricyclic Peptide PCSK9 Inhibitors. *J Med Chem* **64**, 16770-16800 (2021). https://doi.org:10.1021/acs.jmedchem.1c01599

11 Sun, H. *et al.* Discovery of Novel Small Molecule Inhibitors Disrupting the PCSK9-LDLR Interaction. *J Chem Inf Model* **61**, 5269-5279 (2021). https://doi.org:10.1021/acs.jcim.1c00521

12 Petrilli, W. L. *et al.* From Screening to Targeted Degradation: Strategies for the Discovery and Optimization of Small Molecule Ligands for PCSK9. *Cell Chem Biol* **27**, 32-40 e33 (2020). https://doi.org:10.1016/j.chembiol.2019.10.002

13 Kuzmich, N. *et al.* PCSK9 as a Target for Development of a New Generation of Hypolipidemic Drugs. *Molecules* **27** (2022). https://doi.org:10.3390/molecules27020434

14 Raal, F. J. *et al.* PCSK9 inhibition with evolocumab (AMG 145) in heterozygous familial hypercholesterolaemia (RUTHERFORD-2): a randomised, double-blind, placebo-controlled trial. *Lancet* **385**, 331-340 (2015). https://doi.org:10.1016/S0140-6736(14)61399-4

15 Chatzigoulas, A. & Cournia, Z. Rational design of allosteric modulators: Challenges and successes. *Wires Comput Mol Sci* **11**, e1529 (2021). https://doi.org:ARTN e1529
10.1002/wcms.1529

16 Ni, D. *et al.* Discovery of cryptic allosteric sites using reversed allosteric communication by a combined computational and experimental strategy. *Chem Sci* **12**, 464-476 (2020). https://doi.org:10.1039/d0sc05131d

17 Leroux, A. E. & Biondi, R. M. Renaissance of Allostery to Disrupt Protein Kinase Interactions. *Trends Biochem Sci* **45**, 27-41 (2020). https://doi.org:10.1016/j.tibs.2019.09.007

18 Ni, D. *et al.* Along the allostery stream: Recent advances in computational methods for allosteric drug discovery. *Wires Comput Mol Sci* **12**, e1585 (2022). https://doi.org:ARTN e1585
10.1002/wcms.1585

19 Berezovsky, I. N. & Nussinov, R. Multiscale Allostery: Basic Mechanisms and Versatility in Diagnostics and Drug Design. *J Mol Biol* **434**, 167751 (2022). https://doi.org:10.1016/j.jmb.2022.167751

20 Toogood, P. L. Inhibition of protein-protein association by small molecules: approaches and progress. *J Med Chem* **45**, 1543-1558 (2002). https://doi.org:10.1021/jm010468s

21 Nussinov, R. & Tsai, C. J. Allostery in disease and in drug discovery. *Cell* **153**, 293-305 (2013). https://doi.org:10.1016/j.cell.2013.03.034

22 Evison, B. J. *et al.* A small molecule inhibitor of PCSK9 that antagonizes LDL receptor binding via interaction with a cryptic PCSK9 binding groove. *Bioorg Med Chem* **28**, 115344 (2020). https://doi.org:10.1016/j.bmc.2020.115344

23 Perez-Hernandez, G., Paul, F., Giorgino, T., De Fabritiis, G. & Noe, F. Identification of slow molecular order parameters for Markov model construction. *J Chem Phys* **139**, 015102 (2013). https://doi.org:10.1063/1.4811489

24 Molgedey, L. & Schuster, H. G. Separation of a mixture of independent signals using time delayed correlations. *Phys Rev Lett* **72**, 3634-3637 (1994). https://doi.org:10.1103/PhysRevLett.72.3634

25 Schwantes, C. R. & Pande, V. S. Improvements in Markov State Model Construction Reveal Many Non-Native Interactions in the Folding of NTL9. *J Chem Theory Comput* **9**, 2000-2009 (2013). https://doi.org:10.1021/ct300878a

26 Kumawat, A., Chakrabarty, S. & Kulkarni, K. Nucleotide Dependent Switching in Rho GTPase: Conformational Heterogeneity and Competing Molecular Interactions. *Scientific Reports* **7**, 45829 (2017). https://doi.org:10.1038/srep45829

27 Kumawat, A. & Chakrabarty, S. Hidden electrostatic basis of dynamic allostery in a PDZ domain. *Proceedings of the National Academy of Sciences* **114**, E5825-E5834 (2017). https://doi.org:10.1073/pnas.1705311114

28 Ma, B., Tsai, C. J., Haliloglu, T. & Nussinov, R. Dynamic allostery: linkers are not merely flexible. *Structure* **19**, 907-917 (2011). https://doi.org:10.1016/j.str.2011.06.002

29 Papaleo, E. *et al.* The Role of Protein Loops and Linkers in Conformational Dynamics and Allostery. *Chem Rev* **116**, 6391-6423 (2016). https://doi.org:10.1021/acs.chemrev.5b00623

30 Motlagh, H. N., Wrabl, J. O., Li, J. & Hilser, V. J. The ensemble nature of allostery. *Nature* **508**, 331-339 (2014). https://doi.org:10.1038/nature13001

31 Tzeng, S. R. & Kalodimos, C. G. Protein dynamics and allostery: an NMR view. *Curr Opin Struct Biol* **21**, 62-67 (2011). https://doi.org:10.1016/j.sbi.2010.10.007

32 Schulze, J. O. *et al.* Bidirectional Allosteric Communication between the ATP-Binding Site and the Regulatory PIF Pocket in PDK1 Protein Kinase. *Cell Chem Biol* **23**, 1193-1205 (2016). https://doi.org:10.1016/j.chembiol.2016.06.017